

Supplementary Materials for
**Structure of the Shaker Kv channel and mechanism of slow
C-type inactivation**

Xiao-Feng Tan, Chanhyung Bae, Robyn Stix, Ana I. Fernández-Mariño, Kate Huffer,
Tsg-Hui Chang, Jiansen Jiang, José D. Faraldo-Gómez, Kenton J. Swartz*

*Corresponding author. Email: swartzk@ninds.nih.gov

Published 18 March 2022, *Sci. Adv.* **8**, eabm7814 (2022)
DOI: 10.1126/sciadv.abm7814

The PDF file includes:

Figs. S1 to S10
Tables S1 and S2
Legends for movies S1 to S3

Other Supplementary Material for this manuscript includes the following:

Movies S1 to S3

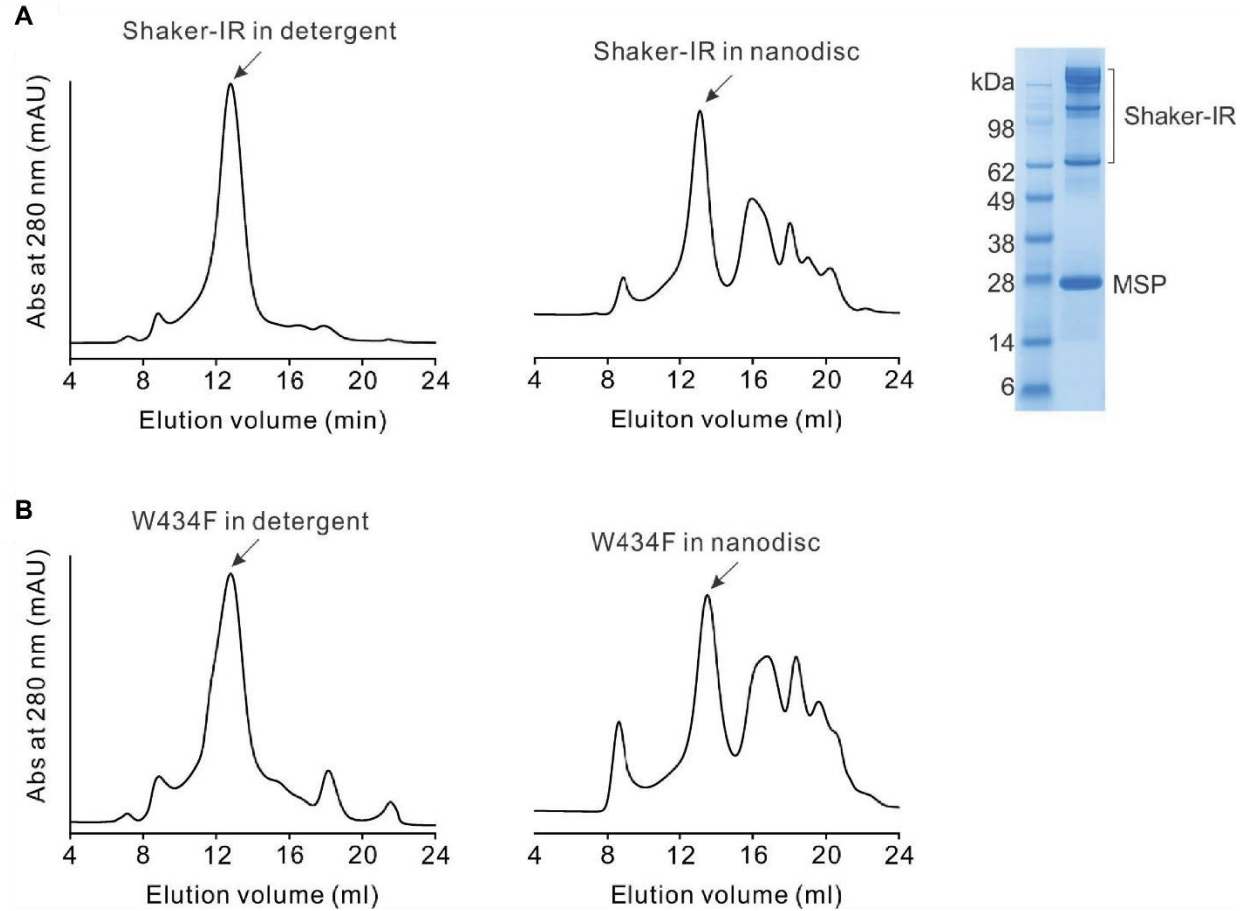
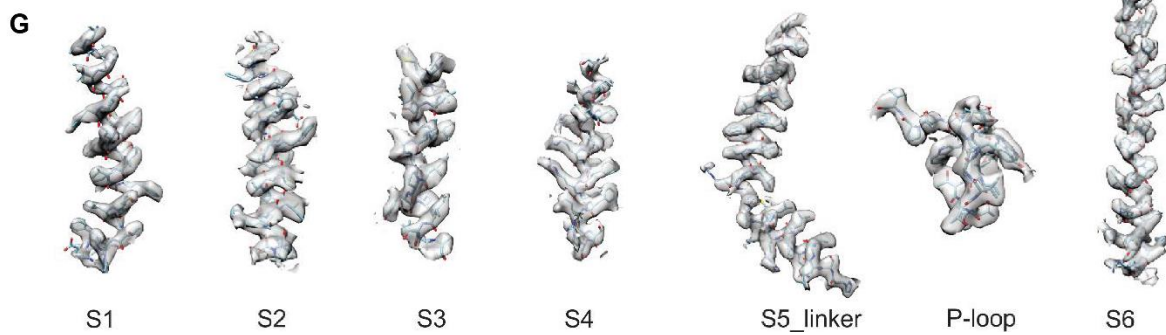
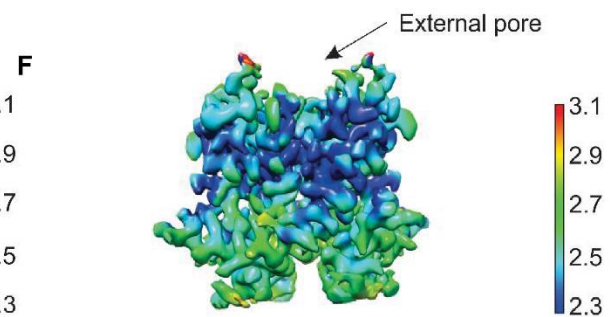
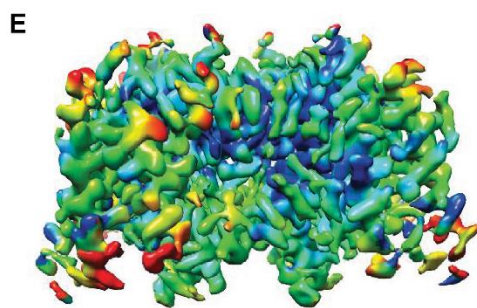
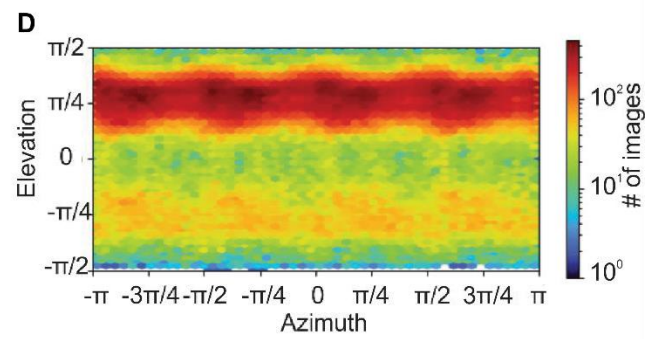
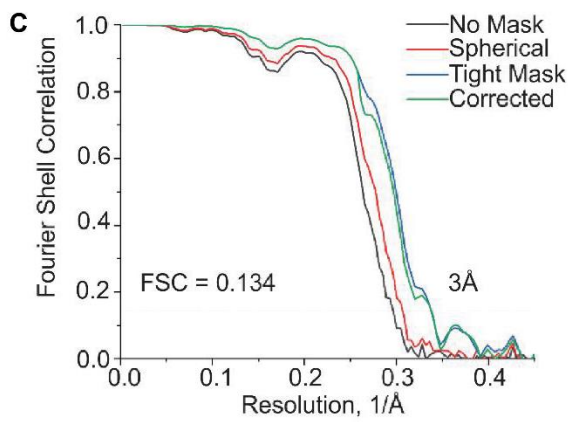
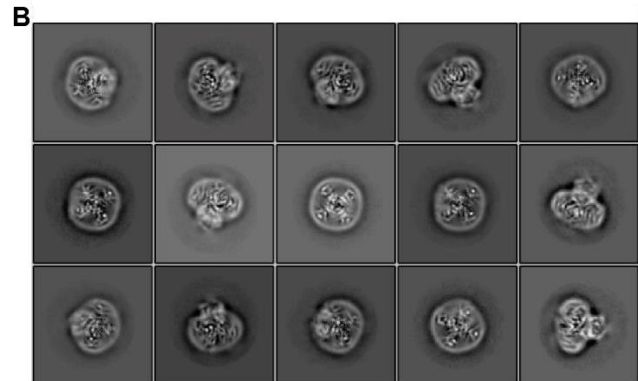
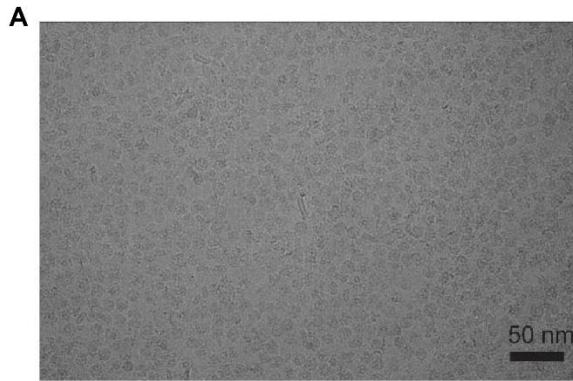


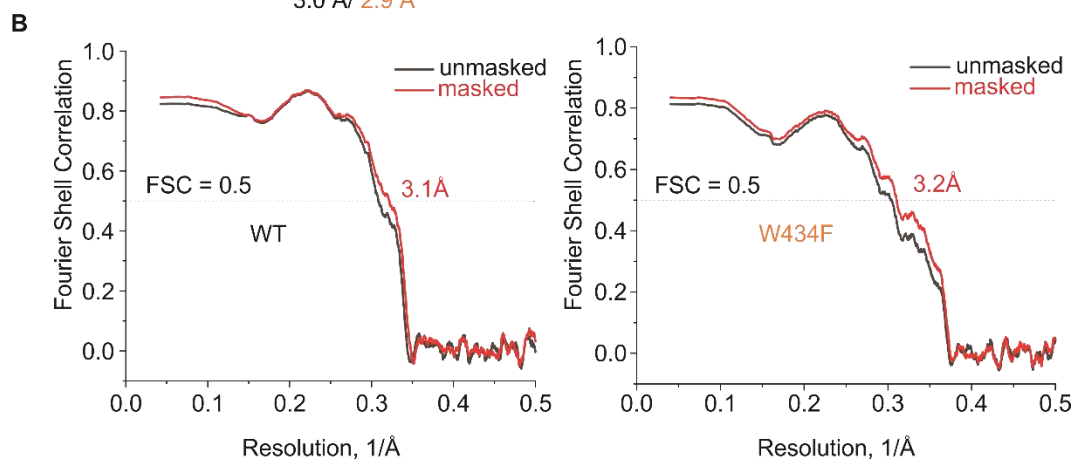
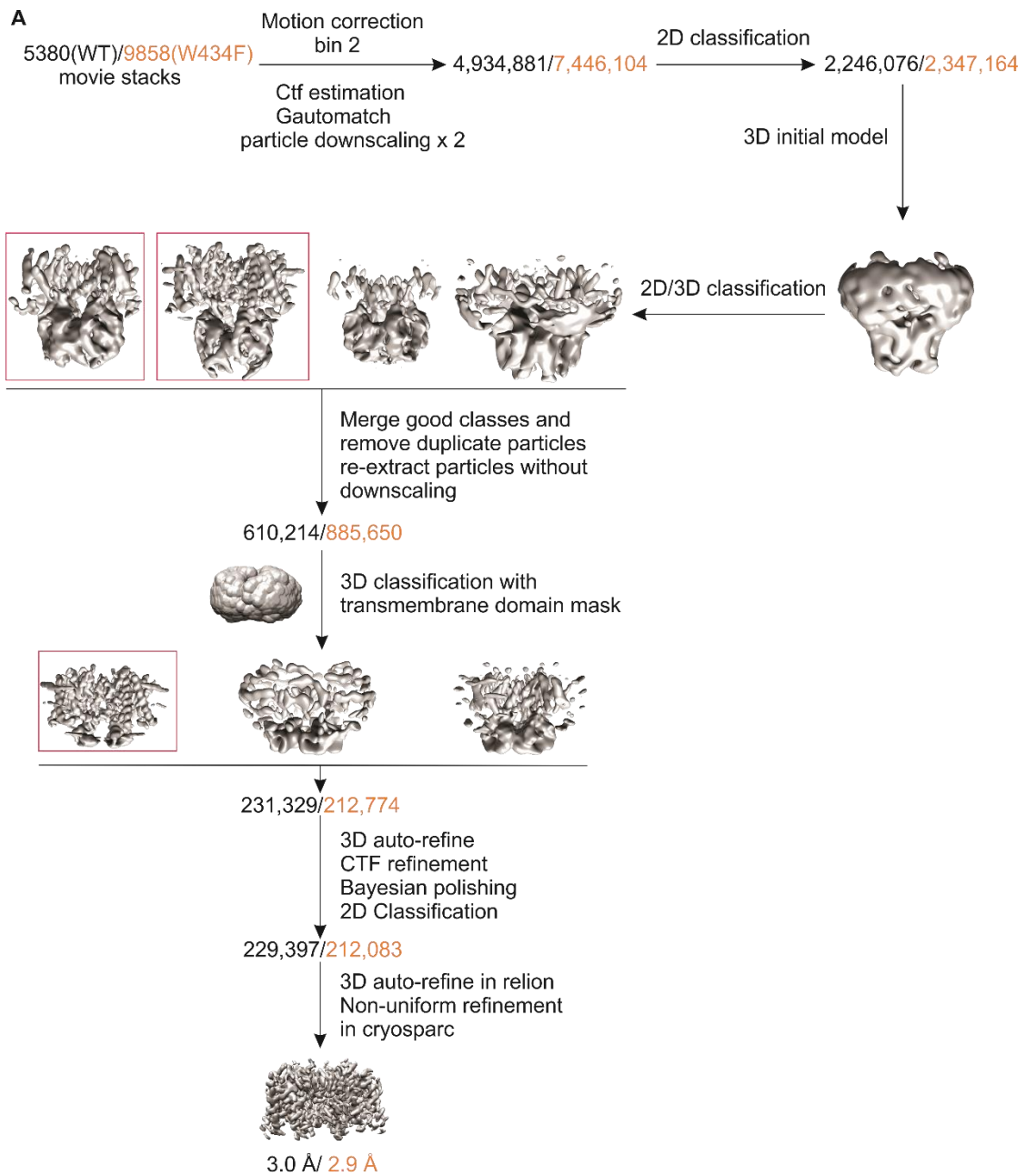
Fig. S1. Biochemistry for wild-type Shaker-IR and W434F mutant.

(A) Gel filtration chromatograms of the Shaker-IR in detergent (left) and in nanodisc (middle), and SDS-PAGE of Shaker-IR in nanodisc. The multiple bands running at a higher molecular weight in the gel correspond to glycosylated species of Shaker. (B) Gel filtration chromatograms of the W434F mutant in detergent (left) and in nanodisc (right). The peak fractions marked with the arrow were collected and used either for nanodisc reconstitution or for cryo-EM imaging.



← **Fig. S2. Cryo-EM imaging of Shaker-IR.**

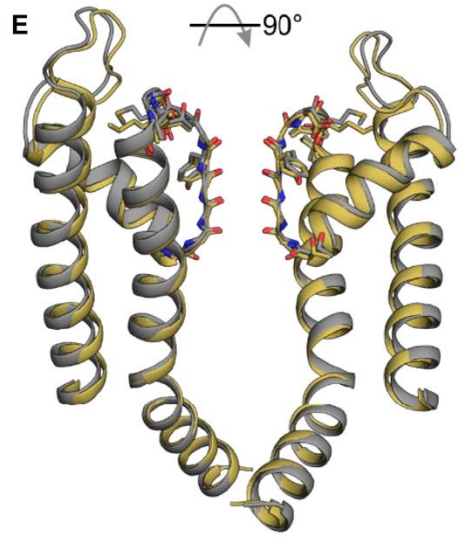
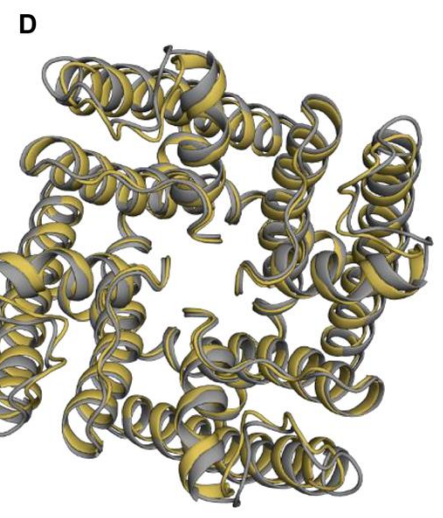
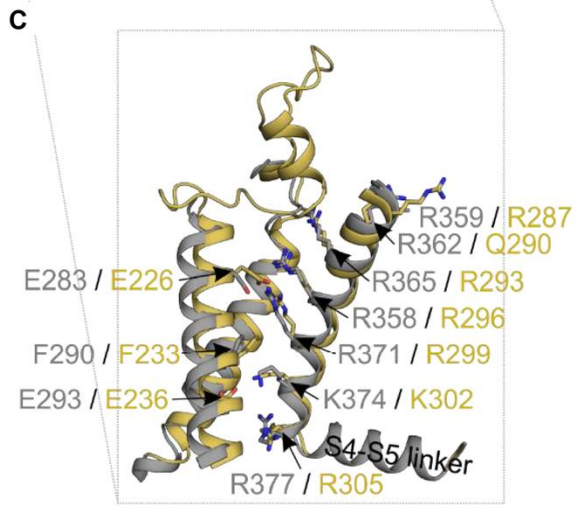
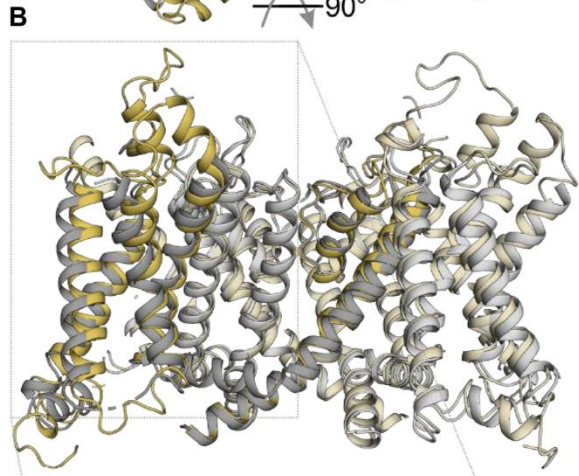
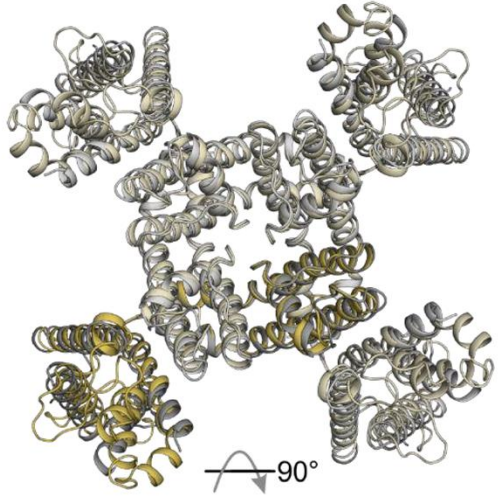
(A) Cryo-EM micrograph of Shaker-IR. **(B)** 2D class averages of the particles in different orientations. **(C)** Fourier Shell Correlation (FSC) curves. **(D)** Direction distribution plots of the 3D reconstruction. **(E)** Local resolution map for the entire TM region. **(F)** Local resolution map for the S5-S6 pore domain, highlighting the dark blue region within the outer pore that shows the best resolution in the overall structure. **(G)** Regional cryo-EM density for Shaker-IR.



← **Fig. S3. Data processing workflow for the cryo-EM structures of Shaker-IR and the W434 mutant.**

(A) Workflow for the cryo-EM data processing. **(B)** FSC curves of the model versus map.

A Shaker-IR
Kv 1.2/2.1 paddle chimera

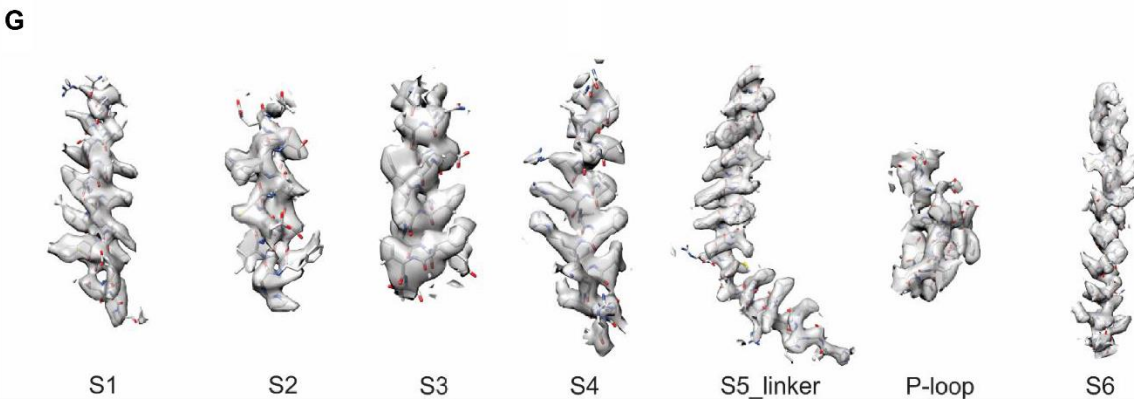
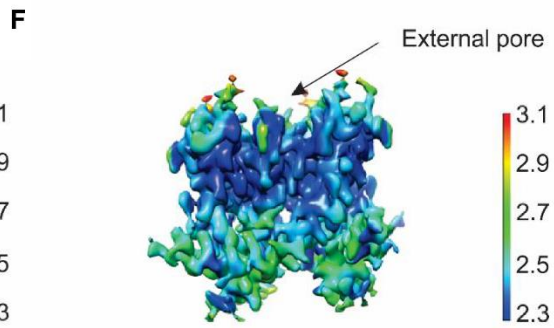
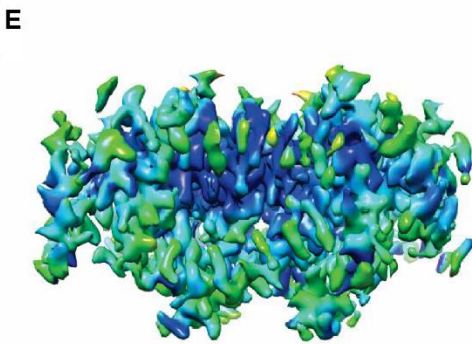
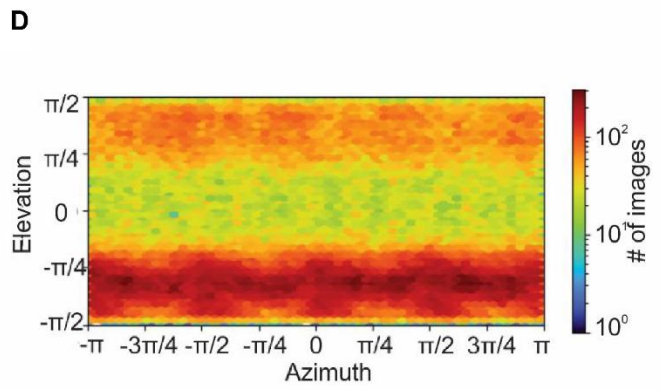
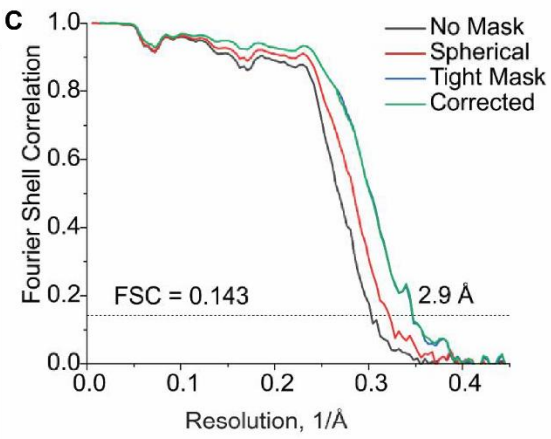
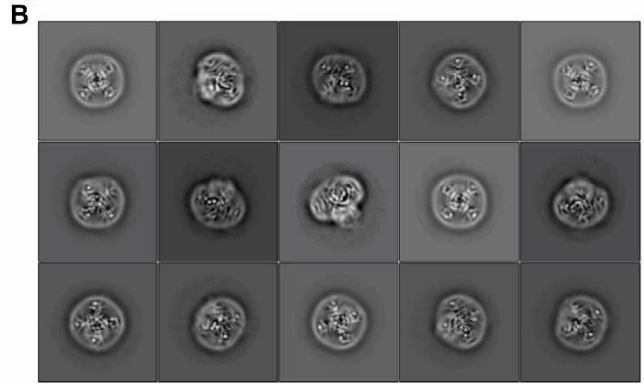
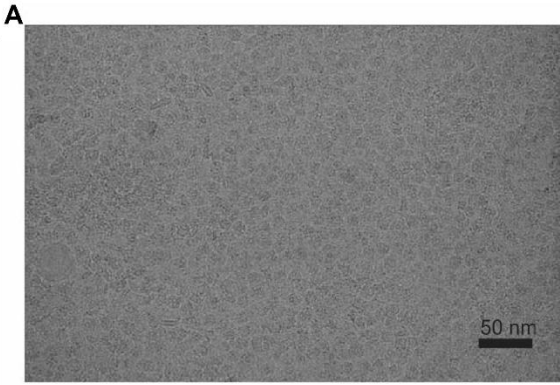


← **Fig. S4. Structural alignment of Shaker Kv channels with the Kv2.1/1.2 paddle chimera.**

Superimposition of transmembrane domains (S1-S6) of Shaker-IR (7SIP) and the Kv 1.2/2.1 paddle chimera (2R9R) **(A)** top and **(B)** side views, along with **(C)** focused view of one S1-S4 voltage- sensing domains with basic residues in S4 and charge transfer center residues shown as sticks. Superimposition of pore domains (S5-S6) **(D)** top and **(E)** side views. Superimpositions of the transmembrane domains (S1-S6) were created using Fr-TM-Align.

← **Fig. S5. Sequence alignment of K⁺ channels.**

Sequence alignment of Shaker (*Drosophila melanogaster* P08510), KcsA (*Streptomyces lividans* P0A334), Kv1.2 (*Rattus norvegicus* P63142), Kv2.1 (*Rattus norvegicus* P15387), Kv1.2/2.1 chimera (*Rattus norvegicus* PDB: 6EBK), Kv3.1 (*Rattus norvegicus* P25122) and Kv4.1 (*Mus Musculus* Q03719). Blue regions indicate similarity and dark blue region indicate identity. Cartoons represent secondary structure features. Green arrows highlight important residues in the charge transfer center and red bar indicates residues that change conformation most dramatically between Shaker-IR and W434F.



← **Fig. S6. Cryo-EM imaging of Shaker W434F.**

(A) Cryo-EM micrograph of Shaker W434F. **(B)** 2D class averages of the particles in different orientations. **(C)** Fourier Shell Correlation (FSC) curves. **(D)** Direction distribution plots of the 3D reconstruction. **(E)** Local resolution map for the entire TM region. **(F)** Local resolution map for the S5-S6 pore domain, highlighting the dark blue region within the outer pore that shows the best resolution in the overall structure. **(G)** Regional cryo-EM density for Shaker W434F.

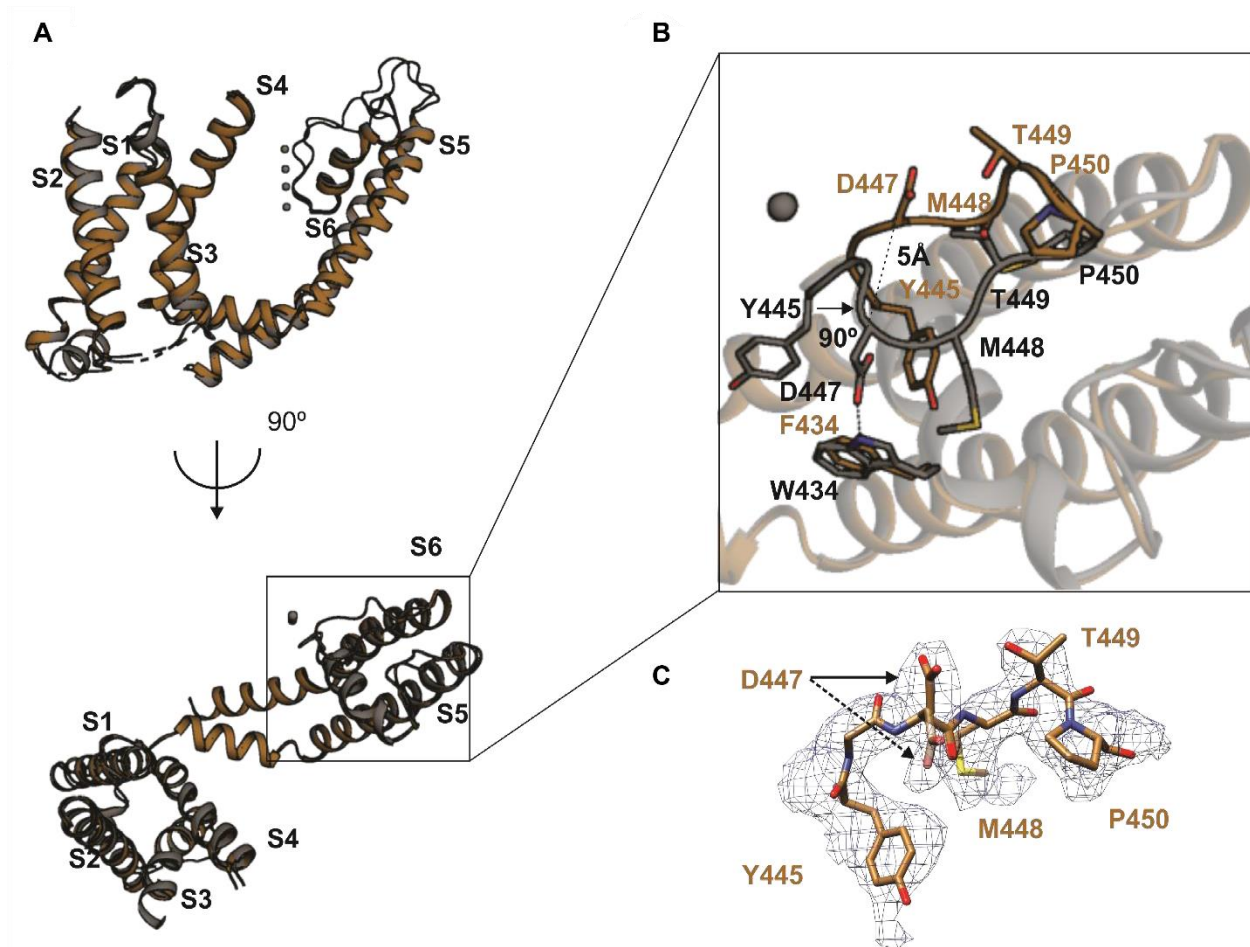


Fig. S7. Structural alignment of Shaker-IR with the W434F mutant.

(A) Superimposition of the Shaker-IR (gray) and W434F (brown) viewed from the side (top image) or from the external side of the membrane (bottom). (B) Close-up view of the conformational change within the outer pore domain viewed from the external side of the membrane. (C) Cryo-EM density of P-loop for the W434F mutant. Density for two distinct rotamers of D447 are indicated by arrows.

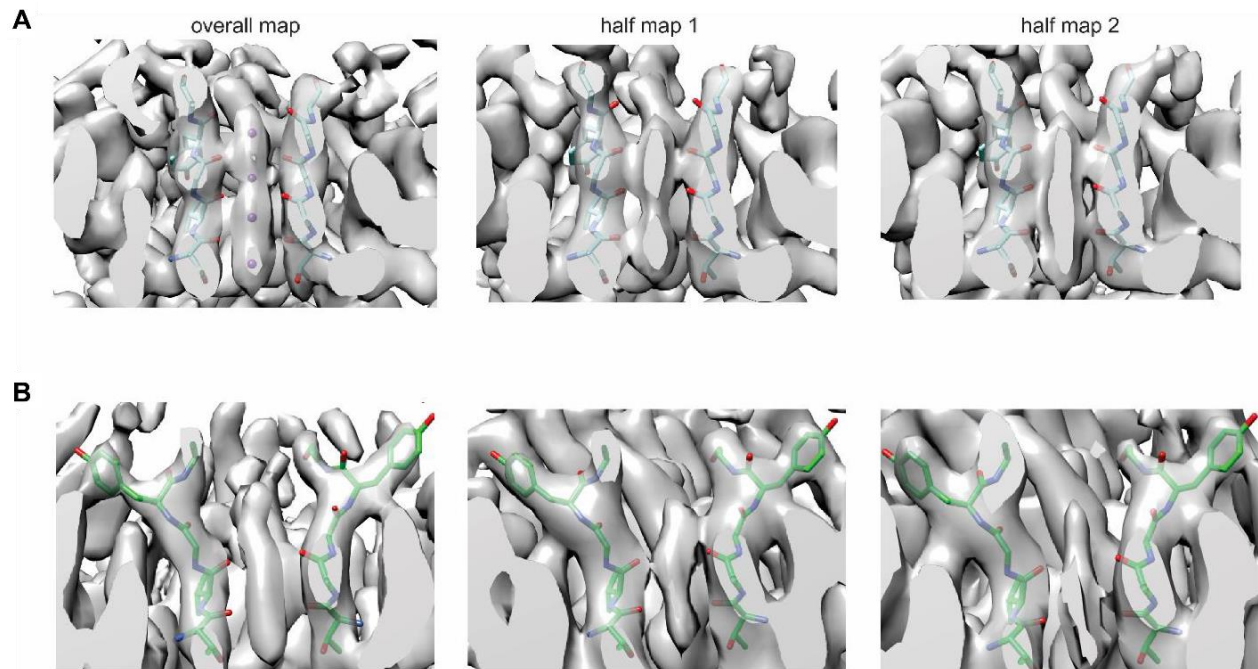


Fig. S8. Ion densities in the selectivity filter of Shaker-IR and the W434F mutant.

(A) Ion density of Shaker-IR using C1 symmetry reconstruction shown in the overall map and half maps (lowpass at 3.5 Å). 4 ions (purple) are fit into S1-S4 sites (left panel), with residues in the filter shown in stick. (B) Ion density of Shaker W434F using C1 symmetry reconstruction for the overall map and half maps (lowpass at 3.5 Å). Cryo-EM density between S1 and S2 sites are much weaker for W434F compared with Shaker-IR.

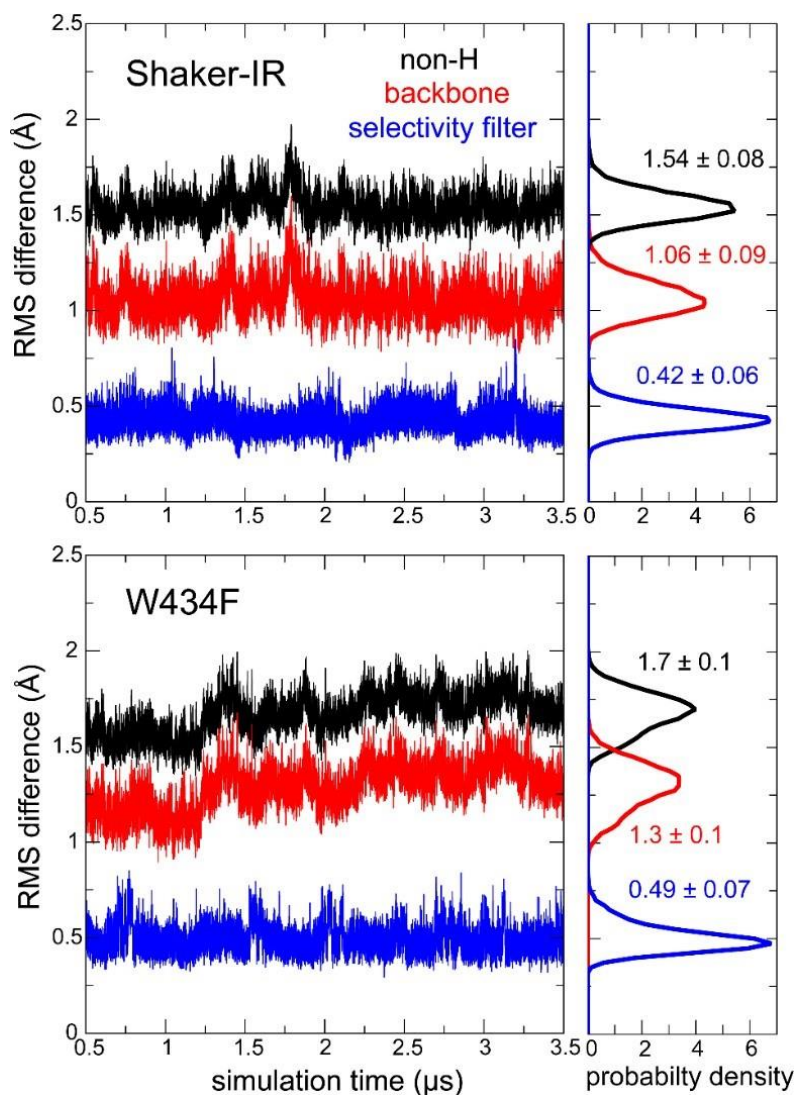
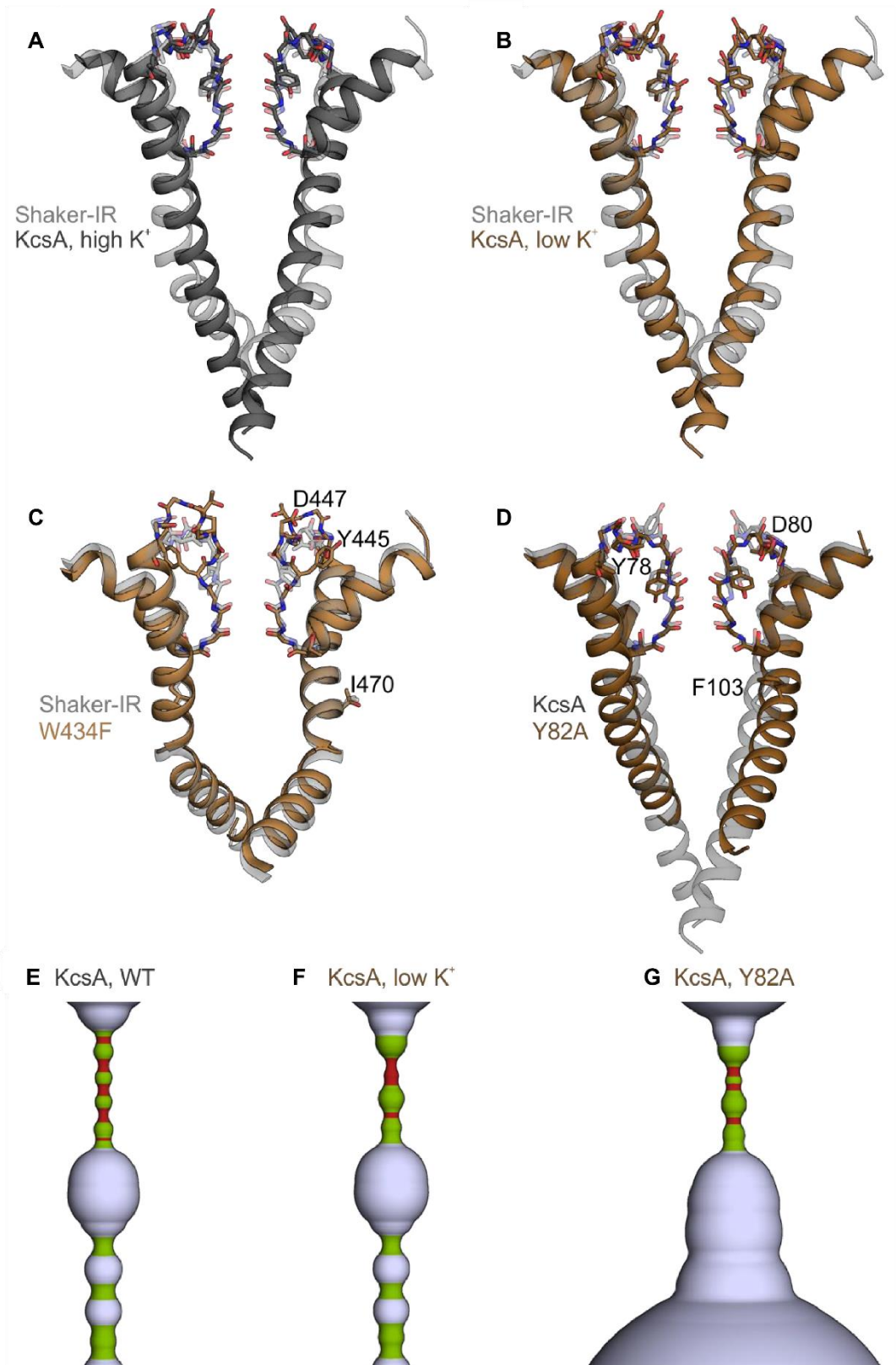


Fig. S9. MD simulations of Shaker-IR and the W434F mutant.

For the portion of the calculated MD trajectories wherein a transmembrane voltage is applied (300 mV for Shaker-IR and 300/450 mV for W434F), the figures on the left side quantify the root-mean-square (RMS) difference between each of the snapshots (in intervals of 120 ps) and the corresponding cryo-EM structure. RMS differences are quantified for all non-hydrogen atoms in the protein structures (black), only for the backbone atoms (red), and only for the backbone atoms of residues 442 to 445. On the right, the figure shows normalized probability histograms of the time-series shown on the left; mean values and standard-deviations are provided in each case.



← **Fig. S10. Comparison of Shaker Kv channel structures with KcsA.**

(A) Superimposition of S6 and pore helix (two opposing subunits) of Shaker-IR (7SIP) and KcsA in the presence of high K^+ (200 mM K^+ , 1K4C). (B) Superimposition of S6 and pore helix of Shaker-IR (7SIP) and KcsA in the presence of low K^+ (3 mM K^+ , 1K4D). (C) Superimposition of S6 and pore helix of Shaker-IR (7SIP) and W434F mutant (7SJ1). (D) Superimposition of S6 and pore helix of KcsA in the presence of high K^+ (1K4C) and the KcsA rapidly-inactivating Y82A mutant (5VKE). Superimpositions of the pore domain (S5-S6) were created using Fr-TM-Align. HOLE diagrams of (E) KcsA in the presence of high K^+ (1K4C), (F) KcsA in the presence of low K^+ (1K4D), and (G) KcsA fast-inactivating Y82A mutant (5VKE). Radii $\leq 1\text{\AA}$ are shown in red, radii $\leq 2\text{\AA}$ and $> 1\text{\AA}$ are shown in green, and radii larger than 2\AA are shown in light blue.

Table S1. Cryo-EM data collection, refinement and validation statistics.

	Shaker-IR (EMDB-25147) (PDB 7SIP)	Shaker-W434F (EMDB-25152) (PDB 7SJ1)
Data collection and processing		
Magnification	105,000	105,000
Voltage (kV)	300	300
Detector	Gatan K3	Gatan K3
Electron exposure (e ⁻ /Å ²)	52	52
Defocus range (μm)	-0.5 to -1.5	-0.5 to -1.5
Pixel size (Å)	0.43	0.43
Symmetry imposed	C4	C4
Initial particle images (no.)	4,934,881	7,446,104
Final particle images (no.)	229,379	212,083
Map resolution (Å)	3.0	2.9
FSC threshold	0.143	0.143
Refinement		
Initial model used (PDB code)	6EBM	6EBM
Model resolution (Å)	3.1	3.2
FSC threshold	0.5	0.5
Map sharpening <i>B</i> factor (Å ²)	-129	-102
Model composition		
Non-hydrogen atoms	7560	6495
Protein residues	892	784
Ligands	36	35
<i>B</i> factors (Å ²)		
Protein	65.23	35.3
Ligand	60.7	28.7
R.m.s. deviations		
Bond lengths (Å)	0.003	0.003
Bond angles (°)	0.508	0.531
Validation		
MolProbity score	1.14	1.43
Clashscore	3.49	7.17
Poor rotamers (%)	0	0
Ramachandran plot		
Favored (%)	98.72	98.01
Allowed (%)	1.28	1.99
Disallowed (%)	0	0

Table S2. Multistep protocol to equilibrate the molecular systems constructed in this simulation study.

Step ^a	1	2	3	4	5	6	7	8	9
Positional restraints ^b (kcal/mol/Å ²)	60	60	15	4	-	-	-	-	-
Distance restraints ^c (kcal/mol/Å ²)	-	-	-	-	4	1	1	-	-
Dihedral Φ , Ψ and χ_1 restraints (kcal/mol/deg ²)	-	-	-	-	16	4	4	4	1
Distance-to-center restraints ^d (kcal/mol/Å ²)	-	-	-	-	60	15	-	-	-
Center-of-mass restraints ^e (kcal/mol/Å ²)	1	1	1	1	1	1	1	1	1
Length of simulation (ns)	1	1	1	1	50	25	25	25	25

^a This protocol was carried out with NAMD 2.13 at 0 mV and preceded the trajectories calculated on Anton2 discussed in the manuscript. All restraints used during the equilibration are harmonic potentials. The table specifies the force constant used for each kind at each step in the protocol.

^b Positional restraints on all non-hydrogen atoms in the protein and on K⁺ and water oxygens in the selectivity filter.

^c Distance restraints on selected hydrogen-bonds and hydrophobic interactions behind the selectivity filter.

^d K⁺ and water molecules were restrained to remain near the geometric center of their designated binding sites in selectivity filter; each center was defined by eight backbone/sidechain oxygens.

^e The protein center-of-mass was restrained to remain near the center of the simulation box.

Movie S1. Morph between the structures of Shaker-IR and the W434F mutant

Movie S2. MD simulation of K⁺ dynamics and permeation through Shaker-IR.

The movie depicts snapshots of K⁺ (magenta, red, purple, yellow, orange spheres) near and within the ion selectivity filter of Shaker-IR (gray cartoon), for a 1- μ s fragment of the trajectory (starting at 1.5 μ s), under 300 mV. Water molecules within 3.8 Å of these K⁺ ions are shown (cyan spheres). The backbone atoms of residues 443-445 and the backbone and sidechain atoms of residue 442 are highlighted (excluding hydrogens).

Movie S3. MD simulation of K⁺ dynamics and permeation through Shaker-W434F.

The movie depicts snapshots of K⁺ (magenta, red, purple, yellow, orange spheres) near and within the ion selectivity filter of Shaker W434F (gray cartoon), for a 1- μ s fragment of the trajectory (starting at 2.0 μ s), under 300 mV for the first 500 ns and under 450 mV for the last 500 ns. Water molecules within 3.8 Å of these K⁺ ions are shown (cyan spheres). The backbone atoms of residues 443-445 and the backbone and sidechain atoms of residue 442 are highlighted (excluding hydrogens).